

**Application of Artificial Intelligence on Quality-Control Tool for Optimum Binder Content  
Determination of OGFC Mixtures**

**Yolibeth Mejias, Senior Project Engineer, Ontario Ministry of Transportation  
Manjriker Gunaratne, Associate Professor and Graduate Coordinator, University of South Florida**

**Paper prepared for presentation at the SES - Testing and Modeling of Road and Embankment  
Materials Session**

**2018 Conference of the Transportation Association of Canada Saskatoon, SK**

**ACKNOWLEDGMENTS:** Author would like to acknowledge the financial support provided by the Florida Department of Transportation (FDOT) through the Contract BDV25, TWO 820-1 and 820-2. The author also recognize and appreciate the personnel of the bituminous section of the FDOT State Material Office (SMO) that provided logistical support and especially the FDOT technicians who provided their expertise and guidance during the testing process of the research.

## ABSTRACT

In some transportation agencies including the Florida Department of Transportation (FDOT) use Open Graded Friction Course (OGFC) mixture to improve skid resistance of asphalt pavements under wet weather. FDOT designs OGFC mixtures using a pie plate visual draindown method FM5-588, which depends on the Optimum Binder Content (OBC) and represents if the mixture has sufficient bonding between the aggregate and asphalt binder, otherwise known as the asphalt binder draindown (ABD). In the FM5-588 the OBC is determined based on visual inspection by trained and experienced technicians. In order to eliminate the human subjectivity involved in aforesaid method, an artificial intelligence (AI) methodology for prediction of the OBC using digital images of the test specimens, perceptual image coding and General Regression Neural Network was created. Then, the author developed a quality control tool (QCT) for the aforementioned AI method to enhance its reliability when implemented by other agencies and contractors. QCT is developed using three quality control imaging parameters of ABD of the test specimen images. In general, this study found that the newly developed AI software provides satisfactory and reliable estimations of OBC and that the QCT will enhance the reliability and accuracy of the AI OBC estimation software.

*Keywords:* Pavement, Asphalt Binder, Image Processing, Human Vision System, quality control, Perceptual Image Coding, Artificial Intelligence, General Regression Neural Network.

## INTRODUCTION

### Objectives of the research

In Florida, all asphalt mixtures are designed by the contractors and submitted to Florida Department of Transportation (FDOT) for review and verification, with the exception of open-graded friction course (OGFC) mixtures. OGFC mixtures are designed by FDOT using the pie plate visual draindown method, FM5-588. In this method, the estimation of the optimum binder content (OBC) is based on a visual assessment of the mixture to ascertain if it has sufficient bonding between the aggregate and asphalt binder, otherwise known as the asphalt binder draindown (ABD), of a set of three mixture samples placed on pie plates with pre-determined trial asphalt binder contents (AC).

In order to eliminate the human subjectivity involved in aforesaid method, the author aims for the following objectives from this research:

1. Developed an artificial intelligence automated image processing-based methodology to predict the OBC of OGFC mixtures using digital images of the test specimens, perceptual image coding and General Regression Neural Network [1].
2. Increased the likelihood of its implementation by other Transportation agencies and contractors alike by using the AI automated method.
3. Generate an associated quality control tool (QCT) for the AI automated method for the aforementioned AI method to enhance its reliability when implemented by other agencies and contractors [2].
4. Aims to optimize the accuracy of the estimated OBC by standardize the pie plate production process.
5. Aims to target values and acceptable tolerances of the identified QCIP for reliability and validity [3 and 4].

### Need for the research

In the US, twenty percent of all DOT agencies have standard procedures for designing OGFC mixtures based on the estimation of OBC. Of them, the common methods are (i) compacted specimens method, (ii) absorption calculation method, and (iii) visual determination method. Approximately ten percent of the aforementioned agencies currently use the visual determination procedure for estimating the OBC of OGFC mixtures. They are Florida (FM5-588), Georgia (GDT114), Nevada (Nev.T760C), New Jersey (NJDOTB-7) and South Carolina (SC-T-90) [5].

The visual OBC determination procedures of the above agencies involve more or less similar general steps. In this process, uncompacted asphalt mixtures are prepared at varying trial AC specific to the aggregate and binder types and placed in clear pie plates for visual inspection of the bottom of the pie plates for the ABD configuration [6]. The preparation of pie plate samples requires heating of the mixture at a specified temperature for a specified period of time. The binder grades, time and temperature at which the mixture is prepared, varies by procedure [5]. The need to **resolve** the constantly encountered **inconsistency issues in predicted OBC results** is essential to assure the accuracy of the OGFC mixture design.

The theoretical framework of the development of an AI automated procedure to estimate OBC of OGFC mixtures and the relevant QC criteria, stems from image processing techniques used in past studies such as aggregate characterization, etc. The **practical implication** of the study is that the implementation of the QC tool will provide technicians and contractors alike to be self-assured that the procedure for OBC prediction of OGFC mixtures is accurate and reliable.

## **EXPERIMENTAL PLAN AND PROCEDURE**

The steps involved in this process are identified in the flowchart seen in Figure 1. Work associated with Phase I and II of the project have been documented in [1, 7, and 8]. Phase I involved the selection of material and preparation of the specimens following FM5-588 while Phase II involved the development of the image-based OBC prediction method. Finally, Phase III consisted of the QCT development process described in detail in this paper.

### **Brief Synopsis of Phase I (Material Selection and Preparation of OGFC Samples)**

Nineteen different OGFC aggregate gradations (mixtures) widely adopted in Florida were selected for testing and evaluation using FM5-588 for determining the OBC of OGFC mixtures. Details of the nineteen project mixtures are shown in Table 1. The aforementioned nineteen mixtures are designated using letters “A” to “S” in this study, for simplicity. The steps involved in this part of the process are identified in the flowchart in Figure 1(a). A brief description of the preparation of specimens for each mixture follows. Two different granitic aggregate sources and two different oolitic limestone aggregate sources were used to create the OGFC mixtures tested using FM5-588. The OGFC gradations of OGFC mix designs comprised a total of 228 samples prepared from 120 granitic and 108 oolitic limestone aggregate sources and PG 67-22 asphalt binder. Hydrated lime was added at a rate of 1.0% by weight of aggregate for each granite mixture, as well as mineral fiber at a rate of 0.4% by total mixture weight for all mixtures, as defined in the FDOT specifications [6, 7 and 8].

FM5-588 requires the preparation of OGFC samples placed in pie plates at three prescribed trial AC based on the aggregate type: 5.3%, 5.8% and 6.3% by weight of total mix for granitic aggregate, and 5.8%, 6.3% and 6.8% by weight of total mix for oolitic limestone aggregate. FM5-588 establishes the OBC of OGFCs based on visual inspection of the bottom of the pie plate specimens for the ABD configuration [6]. This inspection is performed by technicians who determine the OBC based on the trial AC of the three pie plates, guided by documented references, as illustrated in Figure 2 [6, 7 and 8].

### **Brief Synopsis of Phase II (Development of the AI Automated Image Processing-based Methodology)**

The methodology incorporated in the AI automated image processing-based OBC prediction is divided into four sections; (i) Image acquisition, (ii) Basic image processing, (iii) Development and evaluation of relevant imaging parameters, and (iv) OBC prediction model. The steps that are involved in this part of the process are identified in the flowchart in Figure 1(b).

#### *Image Acquisition*

FDOT’s customized imaging system developed to automate the FM5-588 method consists of a standard digital camera (14.1 mega pixels) attached to a custom made aluminum bracket oriented at 35° to the horizontal to minimize glare on the surface during image acquisition. A preliminary computer program developed by FDOT was used to calibrate the pie plate image [1 and 9]. A “dot matrix” calibration unit with a fixed spacing was used in the above setup to calibrate the specific software for the camera angle and simulate an image perspective of a 90° bird’s eye view. The known dimensions of the bracket leg are used to convert pixel values into actual distances during image processing [1 and 9].

### *Basic Image Processing*

A research study by Zelelew, Papagiannakis, and Masad, 2008 [10] introduced an automated digital image processing technique for analyzing the internal structure of asphalt mixtures from CT images. Such innovations for easing the complexity of processing and analysis of the captured images have become acceptable techniques for basic image processing. *Matlab™* was used to implement the different stages of this technique in the current research based on (i) removing the random noise in the image; (ii) converting the grayscale image into a binary image using an appropriate threshold value; (iii) finding the connected components (groups of black pixels) in each image, denoted as “regions”; (iv) assigning a unique label to each identified region; and (v) computing geometric properties of each labelled region [1].

The grouping of connected black pixels into regions was accomplished using the Adjacency Searching Method [11], allowing the connected black pixel regions which are considered to represent the ABD, to be evaluated further. Once the basic processing of images was completed, the AI algorithm proceeds to the parameter analysis stage. A brief discussion of these imaging parameters is found in the next sub-section [1].

### *Development and evaluation of relevant imaging parameters*

Based on the study of visual masking concepts [12], the visibility of the target (ABD regions in the image) in contrast to the mask (rest of the pie plate surface) can be represented by the following parameters related to the surface appearance in each image of pie plates: (i) percent of black pixels of pie plate, (ii) connectivity of black pixels, (iii) number of regions of pie plate, and the averages of the parameters of (iv) orientation, (v) average area of regions, (vi) average perimeter, (vii) uniformity radial, (viii) uniformity angular, (ix) inconsistency coefficient, (x) centroid distance, (xi) form factor, (xii) compactness, (xiii) solidity and (xiv) eccentricity, for the entire PPS image [1].

### *OBC Prediction Model*

To accomplish the automation of the FM5-588 procedure (Phase II), the author analytically modeled the AI perceptual transfer process which involves the two modes of information processing i.e. visual processing and neural processing, performed by the technicians in executing the existing FM5-588 methodology. In developing a quantifiable optical transfer process, the human (technician) visual system (HVS) properties involved in the OBC determination were examined first and a set of relevant imaging parameters was derived out of the above parameters [1].

The chosen imaging parameters and visual OBC estimates from Phase I were then used in designing an AI neural transfer process that would determine the corresponding OBC with minimum human intervention. A General Regression Neural Network (GRNN) was used to uncover the nonlinear correlation between the selected parameters of pie plate images, the corresponding AC and the visually estimated OBC [1].

## **Phase III (Development of Image-based Quality Control Tool, Detailed Description)**

This section provides a detailed discussion of the image-based quality control tool (QCT) development process. It is also intended to provide guidelines on (i) “How to develop” and (ii) “How to evaluate” the image-based QCIP to be used in the QCT. The steps that are involved in this part of the process are identified in the flowchart in Figure 1(c).

The “How to develop” section describes the procedure of producing pie plates of OGFC mixtures currently followed by FDOT using FM5-588. A primary objective of the research effort described in this paper is to identify the specific QCIP from the broad set of imaging parameters listed in previous sections and assess and set up the base actions and quality control standards on the preparation of

pie plates for FM5-588. Meanwhile, the “How to evaluate” section describes methods of identifying and analyzing the ABD characterization by means of the previously identified QCIP. The above analysis is based on the findings of past research studies on aggregate characterization. This section also describes the statistical validation of the QCIP including setting up of the target value and acceptable tolerance for each QC parameter following the measure evaluation criteria [3] that provide a scientific basis for the selection of target values and acceptable tolerances.

#### *“How to Develop” the Image-based QC Parameters*

In FDOT, QC check standards are currently unavailable for the production of pie plates using FM5-588. Consequently, in this study, the following guidelines for checking the production quality of the pie plates were set up by inspecting more than 228 production PPS and consulting with the FDOT Materials office collaborators consisting of the project managers, laboratory technicians, and engineers [13]. The algorithm used for formulating the QCT redefines connected black pixel regions as ellipses with clearly demarcated major and minor axes. An example of an acceptable pie plate image where the black pixels regions are modified as ellipses is shown in Figure 3(a) [3 and 13].

Based on the FDOT Materials Office collaborators’ judgment, a pie plate would become unacceptable due to the following three reasons [13]:

(a) If the PPS has been “slid,” “moved,” or “glided” during the placing of the mixture from the mixing bowl into the pie plate or during the removal of the pie plate from the oven, the ABD’s will show a definitive alignment at a specific angle. An example of an image of a pie plate with such a “slide” is shown on the right side of Figure 3(c), while an image of a pie plate with “no slide” is shown on the left side of Figure 3(b).

(b) If the PPS has been “dropped,” “dumped,” or “forced into place” during the placing of the mixture from the mixing bowl into the pie plate, the ABD will be displayed as an uneven distribution over the bottom surface of the pie plate. An example of an “unevenly distributed” ABD is shown on Figure 3(e), while an “evenly distributed” ABD is shown on Figure 3(d).

(c) If the PPS has been left with “aggregate particles not thoroughly coated” or with “large conglomerates of fines particles” during the mixing of the aggregate batch and free-standing asphalt binder in the mixing bowl, then when the mixture is transferred from the mixing bowl into the pie plate, ABD will exhibit an irregular distribution causing segregation on the outside or the inside of the pie plate. An example of an image of an “incorrectly mixed and segregated” pie plate is shown on Figure 3(g), while a “non-segregated” pie plate image is shown on Figure 3(f).

Following constant communication with FDOT collaborators regarding the PPS production, the current lightly adopted visual QC checks were reviewed and a set of three relevant, definitive and measurable QCIP that would represent the technician’s visual QC checks in a more systematic and objective manner, were selected from the broad set imaging parameters previous subsection. These three parameters address the following specific properties of ABD of PPS; (i) orientation, (ii) spatial distribution, and (iii) segregation [13].

#### *“How to Evaluate” The Image-Based QC Parameters*

This section describes the (i) evaluation of QCIP using findings of past aggregate characterization research studies [14 to 20], and (ii) statistical analysis of QCIP obtained from Phase III of the study to demonstrate their applicability, and [3] simulation and statistical studies for determining the QC standards including the target values and acceptable tolerances of the selected QCIP. Figure 3 and Figure 4 illustrates the QCIP and the following section describes in detail, the methodology used to evaluate the QCIP.

### Evaluation of QC Parameters

Findings from one of the most complete studies [14] on defining internal aggregate parameters derived from images were used to analyze the ABD regions of the PPS digital images. The steps of redefining the ABD regions into ellipses is shown in Figure 3(a). Major and minor axes of ABD regions are essential for quantifying the QCIP. The major axis of a given ABD region is the line joining two pixels on the boundary contour that are the farthest apart and the length of that line is defined as the major axis length. On the other hand, the minor axis is the longest line perpendicular to the major axis that can be inscribed within that ABD region and its length is the minor axis length. For each ABD region, the aforementioned QCIP are calculated.

**Orientation:** The set of orientation parameters of each ABD region can be defined using two criteria; (i) the orientation angle of the major axis with respect to the horizontal axis ( $\theta_f$ ) and (ii) the orientation angle of the major axis relative to the line joining the centroid of the region to the pie plate center ( $\theta_o$ ) [14, 18 to 19]. Figure 4a) shows the orientation of connected black pixel (ABD) regions of the PPS image expressed using both the above criteria and calculated using equations (1) and (2) respectively.

$$\theta_f = \tan^{-1} \frac{(y_i - y_j^c)}{(x_i - x_j^c)} \quad (1)$$

$$\theta_o = \cos^{-1} \frac{(x_j^c - x^p) + \tan \theta_f (y_j^c - y^p)}{\sqrt{1 + (\tan \theta_f)^2} + \sqrt{(x_j^c - x^p)^2 + (y_j^c - y^p)^2}} \quad (2)$$

where  $x_j^c$  and  $y_j^c$  are the coordinates of the centroid of the labelled region  $j$ ;  $x^p$  and  $y^p$  are the coordinates of the center of the pie plate;  $x_i$  and  $y_i$  are the coordinates of the surface pixel at the outer intersection of a given ABD ellipse and its major principal axis. It must be noted that when  $\theta_f = 90^\circ$ ,  $\theta_o$  must to be calculated using  $\theta_o = \cos^{-1}(y_j^c - y^p)$ .

The next step is the determination of the directional distribution of ABD by calculating the vector magnitude ( $\Delta_f$ ), which quantifies the average anisotropy of the orientation parameters ( $\theta_f$ ) [14]. The aforesaid directional distribution of the ABD vector magnitude is calculated using equation (3) [14 and 17]. The results of directional distribution of the ABD indices ( $\Delta_f$ ) for all PPS tested in Phase I are tabulated in Table 2(a).

$$\Delta_f = \frac{1}{M} * \sqrt{(\sum_{i=1}^M \cos 2\theta_f)^2 + (\sum_{i=1}^M \sin 2\theta_f)^2} \quad (3)$$

where  $\Delta_f$  is the directional distribution of the ABD vector magnitude for the orientation, and  $M$  is the number of  $\theta_f$  values in a given pie plate.

**Spatial Distribution:** The spatial distribution ( $SD$ ) is calculated by first dividing the PPS image into wedge sections as illustrated in Figure 4(b). Several alternative wedge sizes were explored to find the size that would offer an adequate number of wedges from each pie plate image while containing disparate information on connected black pixels within them. Wedges subtending thirty degree angles at the pie plate image center were found to be the optimum for this study. Thus, 12 wedge shaped sections covered the entire cross section of each PPS. Then, an algorithm was developed to evaluate the percentage of ABD with centroids within each section ( $SD_{section}$ ), using Equation (4) [1, 15, 16, and 20]. The presumption underlying the eventual analysis is that, if the ABD regions are evenly distributed in the PPS, then different sections should have more or less identical ABD areas.

The pie plate spatial distribution ( $SD$ ) parameter was calculated as the standard deviation of the  $SD_{section}$  in the twelve sections using Equation (5). Table 2(b) shows the results of the  $SD_{section}$  parameter by section and by pie plate for each PPS used in this study.

$$SD_{section} = \left[ \frac{\text{connected SABD regions in the } \theta=30^\circ \text{ section}}{\text{total connected SABD regions in the pie plate}} \right] * 100 \quad (4)$$

$$SD = \text{Standard Deviation } (SD_{section 1-12}) \quad (5)$$

**Segregation:** Segregation ( $S$ ) is calculated by first dividing each PPS into two sections in the radial direction; the outer section ( $S_o$ ) and the inner section ( $S_i$ ) of the PPS image which are of equal areas as illustrated in Figure 4(c) [18, 19 and 20]. The parameter  $S$  is evaluated by determining the percent of ABD regions with centroids within each of the two sections, using Equation (6) and the ratio of the ABD regions (inner/outer) is evaluated using Equation (7). Table 2(c) shows the results of the segregation distribution and the ratio between the inner and outer section for each PPS used in this study [20].

$$S_{o \text{ or } i} = \left[ \frac{\text{Connected SABD regions in the outer or inner section}}{\text{Connected SABD regions in the pie plate}} \right] * 100 \quad (6)$$

$$S = \left[ \frac{\text{Connected SABD regions in the inner section}}{\text{Connected SABD regions in the outer section}} \right] \quad (7)$$

#### *Statistical verification of quality control imaging parameters (QCIP) and Simulation studies for determining the QC standards*

All the pie plate samples (PPS) used in this study had satisfied the visual quality checks routinely performed by the FDOT technicians. Thus, the above PPS provided a basis for verifying the applicability of the QCIP selected by the author. Consequently, a statistical study was performed on the QCIP computed for all the PPS tested in Phase I of the study. Statistical results were used to establish target values and acceptable tolerances of each QCIP and guidelines for the use of QCIP were formulated.

The three imaging parameters (measures) defined above which are considered as potential QC parameters for the QCT were evaluated by the author against the two scientific acceptability of measure criteria; reliability and validity. Reliability demonstrates that the measure data elements are repeatable, producing the same results a high proportion of the time when assessed in the same population in the same time period and/or that the measure score is precise and validity demonstrates that the measure data elements are correct and/or the measure score correctly reflects the quality of care provided, adequately identifying differences in quality [3].

In the expanded study, a sample set of computer-generated defective pie plates were produced using a computer algorithm to supplement a limited number of defective pie plates prepared by FDOT staff (just one of PPS of the set is defective). In both sets of defective pie plates; computer-generated and those prepared by FDOT staff, the ABD areas were represented by ellipses. Then, QCIP of both sets were evaluated. The statistical results of this set of defective pie plates are shown in Table 4.

**Orientation:** Theoretically, the values of the orientation parameter  $\Delta_f$  range from 0 to 1 with 0 representing a completely random distribution of ABD regions and 1 representing ABD regions that are perfectly aligned in one direction. Table 3(d) shows the statistical t-test results for  $\Delta_f$  parameter obtained from the PPS samples tested in Phase I. Based on the t-test, it was found that the mean

difference of the  $\Delta_f$  parameters within all PPS is 0.119 at a significant level of 99.9%. Based on those results (See Tables 2 and 4) and the scientific acceptability of measure criteria [3], the author propose that the range of  $\Delta_f$  of 0 to 0.25 be considered as the range for acceptable orientation of ABD in a pie plate sample.

**Spatial Distribution:** Theoretically, the value of  $SD_{section}$  for each section should be 8.33 for a perfectly uniform distribution of ABD in the 12 sections of the pie plate. Table 3(b) shows the statistical t-test results for the pie plate spatial distribution ( $SD_{pie\ plate}$ ) parameter for PPS produced in Phase I. Based on the results, it can be seen at a confidence level of 95% that the standard deviation of the spatial distribution is within 0 and 1.52 for acceptable pie plates. The author propose that if the standard deviation of the SD values (See tables 2 and 4) of the 12 sections of the pie plate is less than 1.52 to be considered acceptable [3].

**Segregation:** Theoretically, both the outer and inner segregation parameters ( $S_o$  and  $S_i$ ) must be equal to 50 for an even distribution with no segregation in either the outer section or the inner section. In other words, the ratio ( $S_{ratio}$ ) of the ABD area (inner/outer) must be equal to 1.0 for an evenly distributed ABD in a pie plate. Table 3(c) shows the statistical t-test results of the segregation parameters for the pie plates used in Phase I. It was found at a confidence level of 99% that for the pie plates produced in Phase I, the  $S_{ratio}$  has a mean value of 0.97. The author propose that the  $S_{ratio}$  (inner/outer) range of 0.51 to 1.34 (See tables 2 and 4) be considered acceptable [3].

## DISCUSSION AND RESULTS

On evaluating each of the QCIP for PPS in the database created in Phase I, the favorable conclusions drawn from the results in Tables 2 and 4 regarding the acceptability of the corresponding PPS were also compared to the conclusions reached from the general observation of PPS of each mixture. Complete agreement of the conclusions seen in this exercise verified the applicability of the derived QCIP. In addition, it also verified the accuracy of the algorithm developed by the author in detecting the orientation, spatial distribution and segregation of the ABD regions of the PPS. Since all of the PPS generated in Phase I were acceptable, the above mentioned supplementary set of PPS consisting of computer-generated defective PPS and poor quality PPS created by FDOT were used to demonstrate that the author' algorithm can also identify the inferior quality of those PPS images. The graphical comparison of all three QCIP obtained from both types of PPS are shown in Figure 4. Based on the results of the above comparisons, the following conclusions can be drawn:

The directional distribution ( $\Delta_f$ ) representing each ABD region of a correctly placed PPS and a computer-generated defective PPS are shown in Table 2(a) and 4(a) respectively. Therefore, the first QC parameter, orientation, which is based on  $\Delta_f$  indicate uniformity of ABD orientation within the PPS in acceptable pie plates. Furthermore, based on Table 2, the values of  $\Delta_f$  for correctly placed PPS range from 0 to 0.25 and it can be concluded that orientations of all ABD regions in PPS tested in Phase I are randomly distributed, and not aligned along any one particular direction. The above observations agree with the observation-based acceptable quality of the pie plates with respect to orientation. On the other hand, the defective PPS where the ABD regions were clearly aligned in one direction indicated values of  $\Delta_f$  greater than 0.25. The above results seem to justify the consideration of the acceptable range of  $\Delta_f$  to be 0-0.25 [3].

The results for the second QC parameter, the spatial distribution (SD) are shown in Table 2 and 4. The results justify the consideration of the acceptable range of the standard deviation of the SD parameter to be 0-1.52 [3].

A sample of the results for the third QC parameter, segregation, is shown in Table 2 and 4. Based on Table 2,  $S_i$  and  $S_o$  values of 50% would indicate that the distribution of ABD within each section (inner and outer) is precisely the same and therefore no segregation had occurred in the PPS tested in Phase I. Based on the range of acceptability of  $S$  values for inner and outer sections and that of the  $S_{ratio}$  to be between 0.51 and 1.34 [19], the results show evidence of segregation in some of the PPS images analyzed in this study. On the other hand, the defective PPS consistently produced values of  $S_{ratio}$  of less than 0.51 and greater than 1.34. Hence it can be concluded that the above specified acceptability range for the  $S_{ratio}$  seems to be reasonable [3].

## CONCLUSIONS

As a supplement to the previously concluded study in which the FM5-588 procedure was AI automated for estimating the OBC of OGFC mixtures using digital images of pie plates, an additional image-based tool for QC of pie plate samples was also developed. This QCT requires a set of selected QCIP to be evaluated from all pie plate images prior to executing the image-based OBC prediction method and compared with the respective QC standards to ensure the reliability in the OBC prediction.

During the execution of this project, first, a method for representing the connected black pixel (ABD) regions on pie plates was formulated, using the specific set of QCIP of orientation, spatial distribution and segregation of the ABD regions in pie plates. Then, the above QCIP were evaluated from PPS of a variety of mixture designs produced using the FDOT visual method, FM5-588. The results indicated that the selected QCIP are adequate for the formulation of quality control criteria for PPS production. The acceptability criteria for the above QCIP that included the respective target values and acceptable tolerances were determined based on (i) PPS tested in Phase I (ii) computer simulation of defective PPS, and (iii) actual pie plates with different degrees of defects with respect to the above QCIP. The author believe that the developed QCT will enhance the reliability of the previously developed AI automated OBC prediction method. The above acceptability criteria should be reviewed and possibly revised when more data becomes available for the respective implementing agency.

## REFERENCES

1. Gunaratne, M., and Mejias de Pernia, Y, 2015. "Final Report BDV25 - TWO 820-2," FDOT, Gainesville.
2. Colin J. L., Mahoney, J.P., and Willoughby, K. A., 2009. "Statistical Assessment of Quality Assurance-Quality Control Data for Hot Mix Asphalt," Washington State Department of Transportation, Seattle, Washington.
3. National Quality Forum, "Measure testing and Scientific Acceptability of Measure Properties," 7 12 2011. [Online]. Available: [http://www.qualityforum.org/docs/measure\\_evaluation\\_criteria.aspx](http://www.qualityforum.org/docs/measure_evaluation_criteria.aspx). [Accessed 22 July 2015].
4. Chen, J.-S., Shiah, M.-S., and Chen, H.-J., 2001. "Quantification of Coarse Aggregate Shape and Its Effect on Engineering Properties of Hot-Mix Asphalt Mixtures," *Journal of Testing and Evaluation*, JTEVA, Vol. 29, No. 6, p. pp. 513–519.
5. Putman, B. J., 2012. "Evaluation Of Open-Graded Friction Courses: Construction, Maintenance, and Performance," Report No. FHWA-SC-12-04. South Carolina Department of Transportation In Cooperation with: US Department of Transportation Federal Highway Administration.
6. Florida Department of Transportation (FDOT), 2009. "Determining the Optimum Asphalt Binder Content of an Open-Graded Friction Course Using the Pie," [Online]. Available: <http://www.dot.state.fl.us/statematerialsoffice/administration/resources/library/publications/fstm/methods/fm5-588.pdf>.
7. Gunaratne, M., and Mejias de Pernia, Y, 2014. "Final Report BDV25 - TWO 820-1," FDOT, Gainesville.
8. Mejias de Pernia, Y., Gunaratne, M., Nash, T., and Musselman, J, 2015. "Preliminary assessment of Asphalt binder content of open-graded friction course (OGFC) mixtures using digital image processing," in *Conference Proceedings and Lectern Section at the Annual TRB*, Washington, DC.
9. Florida Department of Transportation (FDOT), 2012. "Test method for Image-based determination of Optimum Asphalt Content of FC-5 mixtures," FDOT State Material Office, Gainesville.
10. Zelelew, H. M.; Papagiannakis, A. T.; Masad, E., 2008. "Application of Digital image processing techniques for asphalt concrete mixture images," in *12th International Conference on Computer Methods and Advances in Geomechanics*.
11. Gonzalez, R.C. and Woods, R. E., 2007. "Some Basic Relationships between Pixels." In: *Digital Image Processing*, Saddle River, NJ; Third Edition, Pearson, pp. 68-71.
12. Pylyshyn, Z., Seeing and visualizing: it's not what you think, 2003. "Seeing and visualizing: it's not what you think." Massachusetts Institute of Technology., Chpt. 2-7.
13. FDOT Materials office collaborators consisting of the project managers, laboratory technicians, and engineers. Personal Communication. State Materials FDOT, Gainesville: 2014-2015.
14. Yue, Z. Q., Bekking, W., and Morin, I, 1995. "Characterization of Aggregates and Quantitatively Study of Asphalt Concrete Microstructure," in *Transportation Research Record 1492*, Washington, D.C, National Research Council, pp. 53-60.
15. Mora, C.F., Kwan, A.K.H., and Chan, H.C., 1998. "Particle Size Distribution Analysis of Coarse Aggregate," *Cement and Concrete Research*, Vol. 28, No. 6, p. p.p. 921–932.
16. Kwan, A.K.H., .Mora, C.F., and Chan, H.C, 1999. "Particle shape analysis of coarse aggregate using digital image processing," *Cement and Concrete research*, pp. p.p. 1403-1410. Elsevier Science Ltd. PII: S0008-8846(99)00105-2.

17. Masad, E., 2003. "The Development of a Computer Controlled Image Analysis System for Measuring Aggregate Shape Properties," Transportation research Board: Final Report for Highway-IDEA Preject 77, Washington State university, Pullman, WA.
18. Bessa, L., Castelo Branco, V., and Soares, J., 2012. "Evaluation of different digital images processing software for aggregates and hot mix asphalt characterizations," Construction and building materials, Issue 37, pp. p.p. 370-378.
19. Hassan, N.A., Airey, G.D., Khan R., and Collop, A. C., 2012. "Nondestructive Characterization of the Effect of Asphalt Mixture Compaction on Aggregate Orientation and Segregation Using X-ray Computed Tomography," International Journal of Pavement Research and Technology, 5[2], pp. pp. 84-92. ISSN 1997-1400.
20. Vadood, M., Johari, M. S., and Rahaei, A.R., 2014. "Introducing a simple method to determine aggregate gradation of hot mix asphalt using image processing," International Journal of Pavement Engineering, pp. 15:2, 142-150, DOI: 10.1080/10298436.2013.786076.

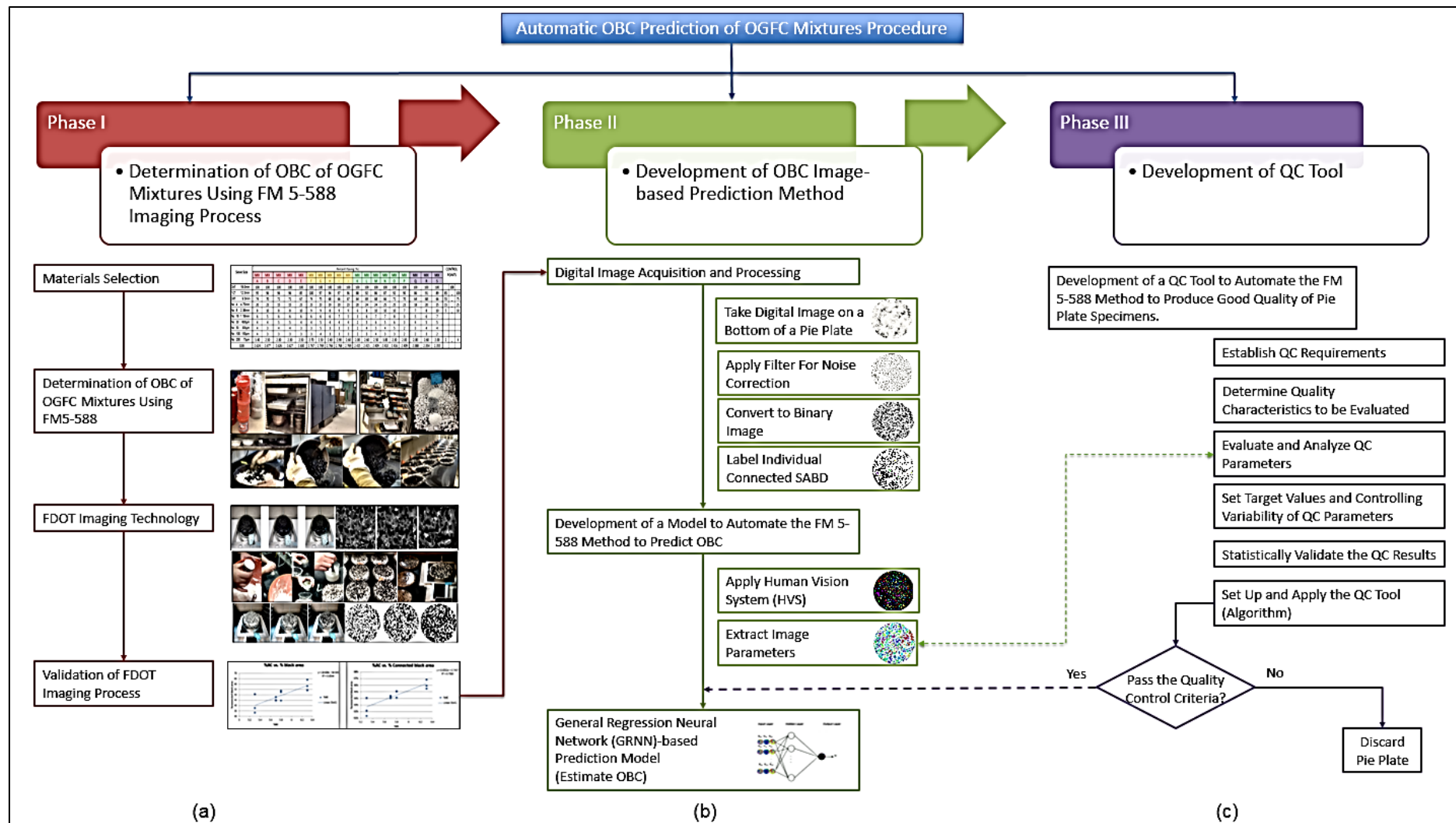


FIGURE 1 Overall framework of research study

TABLE 1 OGFC Gradations Used for the Study

Sieve Size	Nova Scotia Granite					Georgia Granite					White Rock Quarries Limestone					Titan America Limestone			CONTROL POINTS		
	Percent Pasing (%)																				
	MIX A	MIX B	MIX C	MIX D	MIX E	MIX F	MIX G	MIX H	MIX I	MIX J	MIX K	MIX L	MIX M	MIX N	MIX O	MIX P	MIX Q	MIX R		MIX S	
3/4" 19.0mm	100	100	100	100	100	100	100	100	100	100	100	100	100	100	100	100	100	100	100	100	100
1/2" 12.5mm	95	96	96	96	85	100	97	94	97	96	88	92	86	87	92	90	86	91	89	85-100	
3/8" 9.5mm	74	70	71	71	67	74	75	68	66	67	64	69	68	66	71	70	64	68	66	55-75	
No. 4 4.75mm	20	23	15	15	23	23	23	19	20	23	20	24	24	25	25	23	18	20	25	15-25	
No. 8 2.36mm	8	10	8	8	10	9	9	8	9	9	6	8	10	10	10	7	7	8	10	5-10	
No. 16 1.18mm	6	5	6	6	6	6	6	6	7	5	3	6	7	7	8	3	5	6	7		
No. 30 600µm	4	4	5	5	4	4	5	4	4	4	2	5	6	5	6	3	4	5	5		
No. 50 300µm	4	3	4	4	3	3	5	3	3	3	2	4	5	4	5	2	3	4	4		
No. 100 150µm	4	3	3	3	3	3	4	3	3	3	2	3	4	3	3	2	2	3	2		
No. 200 75µm	3.40	2.50	2.30	2.30	2.50	2.70	2.50	2.40	2.90	2.60	2.00	2.60	2.50	3.00	2.30	2.00	2.00	2.60	2.00	2-4	

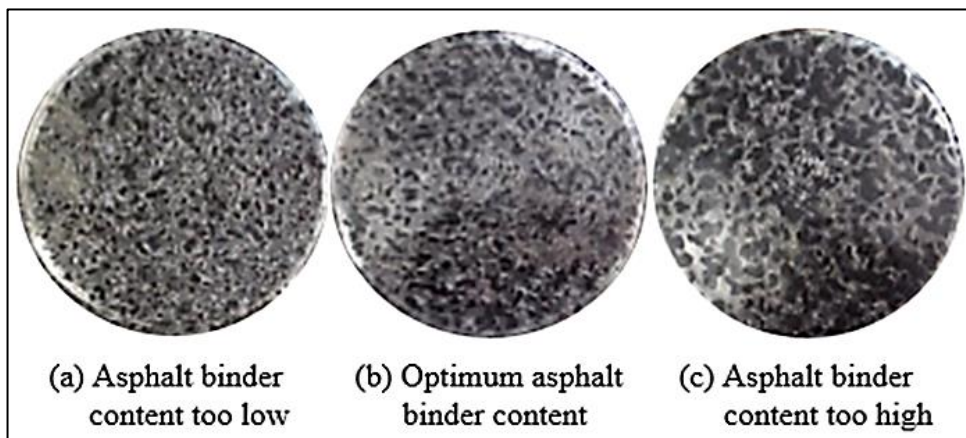


FIGURE 2 Example references for visual inspection of ABD distribution [6]

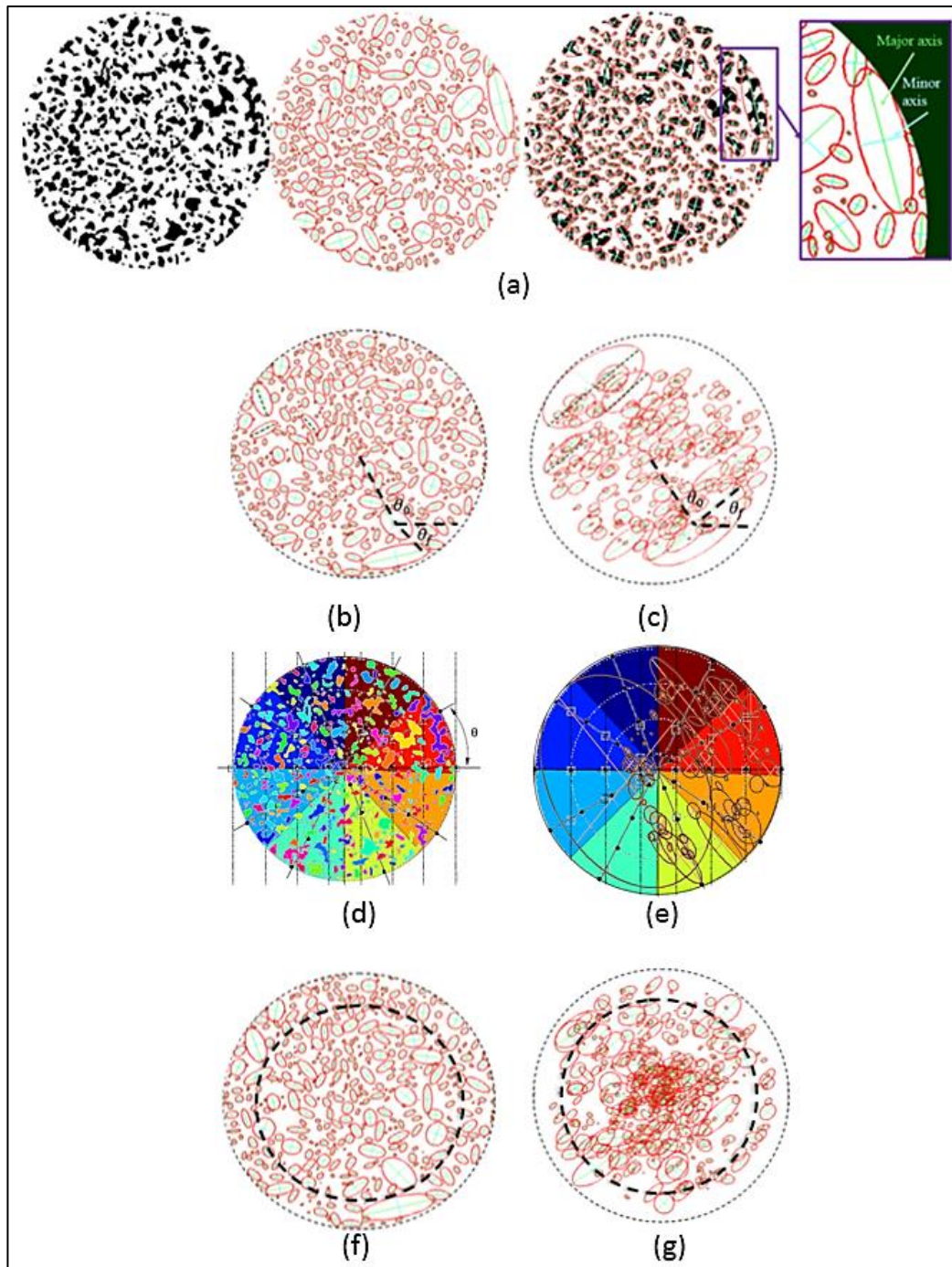


FIGURE 3 Computer-generated images of (a) steps to create ellipses representing the connected black pixel regions of a PPS (b) uniformly distributed PPS, (c) slid (unevenly distributed) PPS, (d) properly placed PPS, (e) incorrectly placed PPS, (f) appropriately mixed PPS, and (g) inappropriately mixed PPS

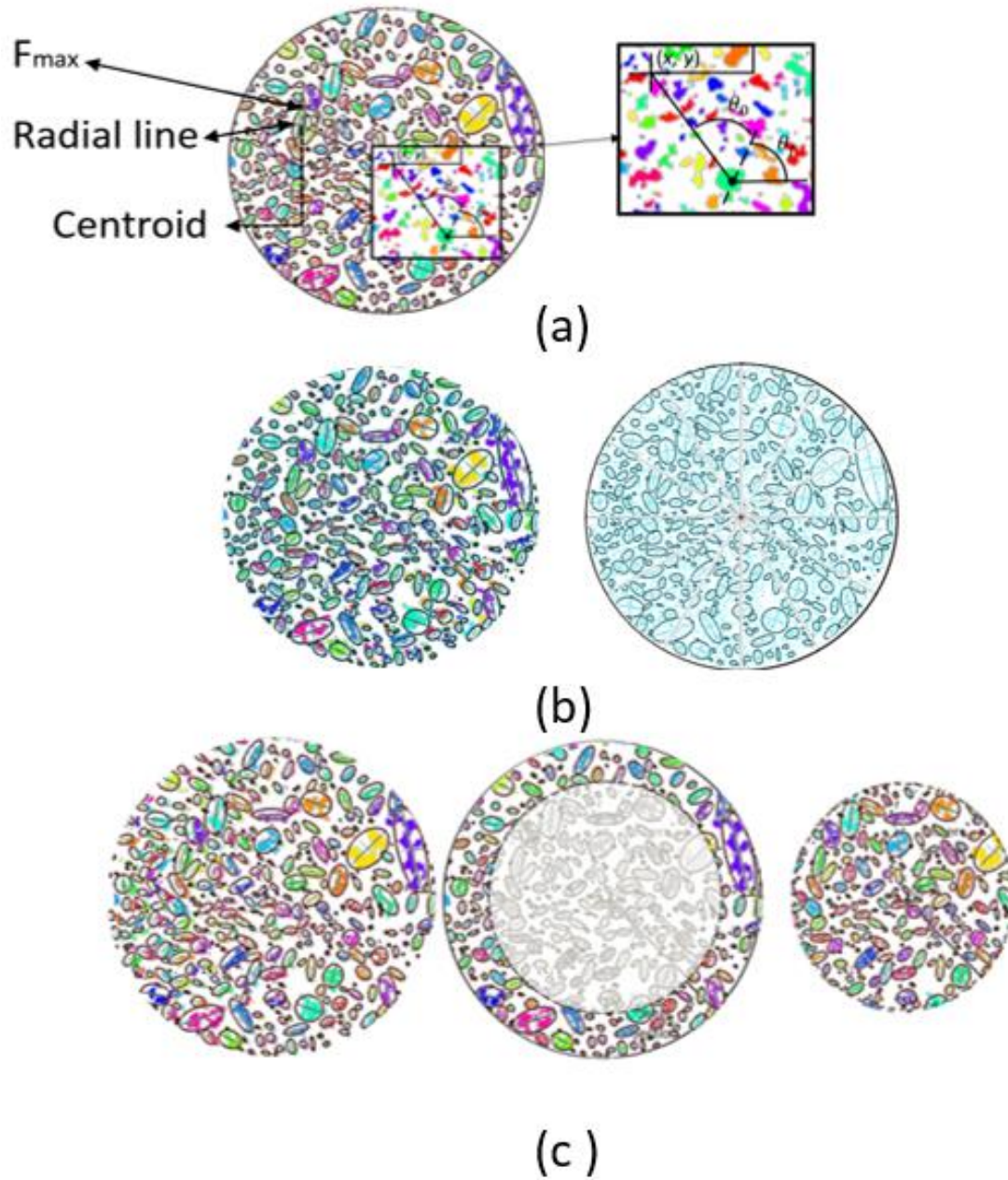


FIGURE 4 Representation of connected black pixels on a pie plate image for ABD identification (a) orientation relative to the center of the pie plate image, (b) location in the angular mesh and (c) illustration of sections of segregation.

TABLE 2 Quality Control Parameter Results for (a) Orientation: Directional Distribution of the ABD ( $\Delta_f$ ), (b) Spatial Distribution (SD), and (c) Segregation (S) Results for Sample Sets for Mixtures "A" to "S"

IMAGE NAME	PERCENT AC	Directional Distribution ( $\Delta_f$ )	Spatial Distribution (SD) by sections of 30 degrees													Spatial Distribution (SD) standard deviation	INNER	OUTER	Segregation	Ratio (inner/outer)
MIX A TRIAL 2.1 5.3%	5.3	0.16	10.54	9.56	8.11	7.76	8.25	9.43	9.31	8.01	6.11	6.08	8.48	8.36	1.32	50.54	49.46	97.86	1.02	
MIX A TRIAL 2.1 5.8%	5.8	0.07	8.92	10.21	7.39	8.46	8.93	9.40	7.77	7.86	7.58	7.59	8.28	7.63	0.88	48.31	51.69	107.02	0.93	
MIX A TRIAL 2.1 6.3%	6.3	0.10	7.86	7.37	8.83	8.39	9.63	9.25	8.88	7.97	7.83	6.72	8.42	8.85	0.82	55.56	44.44	80.00	1.25	
MIX B TRIAL 1.1 5.3%	5.3	0.07	8.78	8.80	7.84	7.94	8.61	8.76	7.52	7.14	9.66	8.15	7.67	9.13	0.74	53.04	46.96	88.52	1.13	
MIX B TRIAL 1.1 5.8%	5.8	0.14	9.06	7.32	7.95	7.64	6.73	7.70	7.56	8.84	10.01	10.18	8.06	8.94	1.07	40.60	59.40	146.32	0.68	
MIX B TRIAL 1.1 6.3%	6.3	0.11	6.99	8.18	7.19	9.05	6.95	7.29	7.96	8.03	9.25	10.17	9.13	9.81	1.12	49.35	50.65	102.63	0.97	
MIX C TRIAL 1.1 5.3%	5.3	0.10	7.93	6.50	7.97	9.27	7.45	9.13	9.83	9.35	9.02	9.41	7.91	6.24	1.18	52.29	47.71	91.24	1.10	
MIX C TRIAL 1.1 5.8%	5.8	0.21	7.73	6.06	7.04	7.13	9.25	8.15	9.25	9.32	8.77	9.92	8.90	8.49	1.14	54.74	45.26	82.69	1.21	
MIX C TRIAL 1.1 6.3%	6.3	0.21	8.14	8.92	7.92	8.15	7.99	7.73	7.72	9.05	10.50	8.93	7.91	7.03	0.90	44.90	55.10	122.73	0.81	
MIX D TRIAL 1.1 5.3%	5.3	0.16	7.51	9.07	8.42	8.80	9.28	8.88	8.70	6.91	8.03	6.33	9.80	8.28	1.00	48.02	51.98	108.26	0.92	
MIX D TRIAL 1.1 5.8%	5.8	0.13	7.52	7.99	7.03	8.13	7.94	6.87	9.84	9.85	9.25	8.54	7.84	9.21	1.01	45.24	54.76	121.05	0.83	
MIX D TRIAL 1.1 6.3%	6.3	0.02	7.73	8.16	7.66	9.33	10.03	9.41	8.78	7.76	7.31	7.18	9.31	7.35	0.99	33.72	66.28	196.55	0.51	
MIX M TRIAL 3.2 6.3%	6.3	0.07	9.38	7.06	7.40	8.20	7.22	7.77	8.53	7.79	8.80	9.29	9.01	9.56	0.88	51.33	48.67	94.81	1.05	
MIX M TRIAL 3.2 6.8%	6.8	0.18	8.73	9.37	7.52	7.01	7.46	7.95	8.08	9.56	8.58	8.57	8.06	9.12	0.80	46.00	54.00	117.39	0.85	
MIX N TRIAL 3.2 5.8%	5.8	0.12	9.69	8.62	10.99	8.53	8.56	7.78	7.27	7.58	7.40	8.48	8.19	6.89	1.13	51.80	48.20	93.05	1.07	
MIX N TRIAL 3.2 6.3%	6.3	0.09	7.89	7.17	7.72	8.32	7.80	8.68	7.48	8.33	8.19	8.94	8.42	11.07	1.00	55.07	44.93	81.59	1.23	
MIX N TRIAL 3.2 6.8%	6.8	0.15	8.69	6.21	9.38	9.29	6.93	7.03	9.24	8.71	9.20	9.99	8.29	7.04	1.22	53.53	46.47	86.82	1.15	
MIX O TRIAL 3.2 5.8%	5.8	0.09	9.09	8.34	8.95	6.36	7.21	9.72	7.44	7.79	8.58	11.10	8.68	6.74	1.33	51.19	48.81	95.34	1.05	
MIX O TRIAL 3.2 6.3%	6.3	0.09	7.14	8.16	7.95	9.15	6.77	8.82	7.51	9.23	8.40	9.32	9.26	8.31	0.87	52.68	47.32	89.82	1.11	
MIX O TRIAL 3.2 6.8%	6.8	0.08	8.27	8.86	8.35	9.05	8.79	9.65	8.89	7.84	6.56	7.70	8.60	7.44	0.84	53.20	46.80	87.96	1.14	
MIX S TRIAL 3.2 5.8%	5.8	0.11	8.82	6.82	8.23	7.47	7.43	9.86	10.47	7.78	8.17	8.60	8.37	7.96	1.02	56.03	43.97	78.46	1.27	
MIX S TRIAL 3.2 6.3%	6.3	0.13	11.07	9.60	9.01	9.15	7.01	8.18	8.21	5.61	8.03	8.12	6.91	9.09	1.42	47.77	52.23	109.34	0.91	
MIX S TRIAL 3.2 6.8%	6.8	0.15	9.34	9.77	7.34	8.70	8.16	6.62	8.88	9.64	7.11	7.53	7.45	9.45	1.10	49.83	50.17	100.67	0.99	

(a)
(b)
(c)

TABLE 3 Statistical “t-test” for the QC Parameters

(a) One-Sample Statistics Statistical t-test for the orientation ( $\Delta_f$ ) parameters

	N	Mean	Std. Deviation	Std. Error Mean
$\Delta_f$	342	.1191	.05243	.00284

	Test Value = 0					
	T	df	Sig. (2-tailed)	Mean Difference	95% Confidence Interval of the Difference	
					Lower	Upper
$\Delta_f$	42.018	341	.000	.11912	.1135	.1247

(b) One-Sample Statistics Statistical t-test for the spatial distribution ( $SD_{pie\ plate}$ ) parameter

	N	Mean	Std. Deviation	Std. Error Mean
$SD_{pie\ plate}$	342	1.0514	.27431	.01483

	Test Value = 0					
	T	df	Sig. (2-tailed)	Mean Difference	95% Confidence Interval of the Difference	
					Lower	Upper
$SD_{pie\ plate}$	70.885	341	.000	1.05143	1.0223	1.0806

(c) One-Sample Statistics Statistical t-test for the segregation ( $S_{ratio}$ ) parameters.

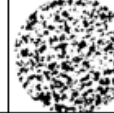
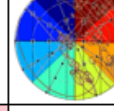
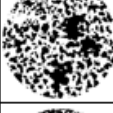
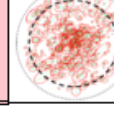
**One-Sample Statistics**

	N	Mean	Std. Deviation	Std. Error Mean
Inner	342	48.3616	7.00167	.37861
Outer	342	51.6384	7.00167	.37861
Ratio	342	.9703	.25737	.01392

**One-Sample Test**

	Test Value = 0					
	T	df	Sig. (2-tailed)	Mean Difference	95% Confidence Interval of the Difference	
					Lower	Upper
Inner	127.736	341	.000	48.36161	47.6169	49.1063
Outer	136.390	341	.000	51.63839	50.8937	52.3831
Ratio	69.720	341	.000	.97028	.9429	.9977

TABLE 4 Results of QC Parameters for Defective Pies Sets

IMAGE NAME	PERCENT AC	QC PARAMETER			IMAGE	IMAGE NAME	PERCENT AC	QC PARAMETER			IMAGE
		ORIENTATION	SPATIAL DISTRIBUTION	SEGREGATION				ORIENTATION	SPATIAL DISTRIBUTION	SEGREGATION	
		$\Delta_f$	Standard Deviation (Section by 30 degrees)	Ratio (inner/outer)				$\Delta_f$	Standard Deviation (Section by 30 degrees)	Ratio (inner/outer)	
MIX 13560	5.3		1.86			MIX 13497	6.8		2.69		
MIX 13560	5.8	0.31		0.47		MIX 13497	6.3		1.85		
MIX 13560	6.3			0.62			5.3	0.32			
MIX 13561	5.8			0.65		COMPUTER GENERATED	5.8		1.85		
MIX 13561	6.3		1.53				6.3			0.62	
MIX 13561	6.3	0.32		0.42							